

# Fast start-up of microchannel fuel processor integrated with an igniter for hydrogen combustion

Shin Kun Ryi<sup>a,b,\*</sup>, Jong Soo Park<sup>b,\*\*</sup>, Song Ho Cho<sup>a</sup>, Sung Hyun Kim<sup>a</sup>

<sup>a</sup> Department of Chemical and Biological Engineering, Korea University, 5-ka, Anam-Dong Sungbuk-Gu, Seoul 136-701, South Korea

<sup>b</sup> Hydrogen System Research Center, Korea Institute of Energy Research, P.O. Box 103, Jang-Dong, Yuseong-Gu, Daejeon 305-343, South Korea

Received 24 March 2006; accepted 7 June 2006

Available online 26 July 2006

## Abstract

A Pt–Zr catalyst coated FeCrAlY mesh is introduced into the combustion outlet conduit of a newly designed microchannel reactor (MCR) as an igniter of hydrogen combustion to decrease the start-up time. The catalyst is coated using a wash-coating method. After installing the Pt–Zr/FeCrAlY mesh, the reactor is heated to its running temperature within 1 min with hydrogen combustion. Two plate-type heat-exchangers are introduced at the combustion outlet and reforming outlet conduits of the microchannel reactor in order to recover the heat of the combustion gas and reformed gas, respectively. Using these heat-exchangers, methane steam reforming is carried out with hydrogen combustion and the reforming capacity and energy efficiency are enhanced by up to 3.4 and 1.7 times, respectively. A compact fuel processor and fuel-cell system using this reactor concept is expected to show considerable advancement.

© 2006 Elsevier B.V. All rights reserved.

**Keywords:** Microchannel reactor; Fuel processor; Proton-exchange membrane fuel cell; Hydrogen combustion; Methane steam reforming; Heat-exchanger

## 1. Introduction

Microchannel reactors (MCR) have attracted much attention on account of their many advantages over other reactors, namely, enhanced heat and mass transfer, flow uniformity, high specific surface-area, safe control in the explosive regime, and easier scale-up without any changes in geometry [1,2]. In recent years, the microchannel reactor has been used for chemical synthesis [3], nanoparticle synthesis [4,5], emulsification for food production [6,7], and medical science [8,9].

In particular, many studies have examined the use of a MCR as a compact fuel processor in fuel cells [10–20]. Microchannels with a high surface-to-volume ratio can improve the rate of heat and mass transfer and enhance the active catalytic reaction rate by as much as 10–500 times that of a conventional reactor and it can dramatically reduce the volume of the fuel processor. A compact size allows the development of a small-scale fuel processor and a portable power generator to replace bat-

tery packs in laptops or mobile phones [11,21]. A typical fuel processor for the steam reforming for PEMFCs is composed of five unit operations such as a fuel preheater, a fuel reformer, a carbon monoxide clean-up process, a heat-exchanger and a combustor. With the merit of microchannel reactors such as the parallel connection of multiple reactors, these five unit operations can be integrated into a single unit. This should enhance the energy efficiency. A combustor for the integrated steam reforming of methane has been developed [10]. Tonkovich et al. [12] developed a steam reformer for the integrated feed preheating and product quenching process. Patil et al. [11] successfully demonstrated a fuel processor that consisted of a vapourizer, steam reformer and heat-exchanger in an entire system. Delsman et al. [18,19] designed and fabricated a heat-exchanger for an integrated preferential oxidation microdevice. The high heat capacity of a microchannel reactor with a metallic plate means, however, that a longer start-up time is required [19].

More desirably, anode-off gases containing hydrogen can be introduced into the combustor as a fuel. The fuel cell typically consumes about 80% hydrogen and the anode-off gas contains about 30% hydrogen. Therefore, there are some changes when using the anode-off gas as a fuel for catalytic combustion. Since hydrogen is extremely light and flows upward across the catalyst

\* Corresponding author. Tel.: +82 42 860 3667; fax: +82 42 860 3309.

\*\* Co-corresponding author. Tel.: +82 42 860 3664; fax: +82 42 860 3309.

E-mail addresses: [shinkun@lycos.co.kr](mailto:shinkun@lycos.co.kr) (S.K. Ryi), [deodor@kier.re.kr](mailto:deodor@kier.re.kr) (J.S. Park).

body [22], there is considerable non-uniformity in the temperature profile of the catalytic bed. Janicke et al. [23] reported hot spots in front of the reactor and some explosion sounds during the test when a  $H_2/O_2$  mixture was introduced in a microchannel reactor with a heat-exchanger. These hot spots and their movement according to the gas flow rates [24] should be carefully controlled in order to apply hydrogen catalytic combustion for hydrocarbon steam reforming. A novel designed microchannel reactor, in which the anode-off gas containing hydrogen could be combusted catalytically, has been developed in a previous study [10]. The start-up time for the reactor was, however, too long for it to be applied to a portable fuel processor. In addition, the energy of combustion and reformed gas had to be recovered.

For these reasons, a FeCrAlY mesh coated with Pt–Zr catalysts has been introduced into the combustion outlet conduit of a novel microchannel reactor as an igniter to decrease the start-up time for hydrogen combustion. The Pt and Zr catalysts are introduced using a wash coating method. A plate-type heat-exchanger is included in order to recover the heat of combustion gas and reformed gas.

## 2. Experimental

### 2.1. An igniter for dynamic process

It was previously reported that a Pt–Sn/ $Al_2O_3$  catalyst coated on a microchannel was sufficiently active to initiate hydrogen combustion at room temperature. A novel microchannel reactor, which was designed to inhibit the formation of hot spots at the mixing point of hydrogen and air, uniformly heated the reactor to  $800^\circ C$  without explosion. Nevertheless, the start-up time to the running temperature of the reactor is approximately 2.5 h. In order to apply this to a portable fuel cell, the start-up time needs to be reduced significantly. Therefore, an igniter, i.e., a FeCrAlY mesh coated with Pt–Zr catalysts, was introduced into the combustion outlet conduit of the reactor reported previously [10]. A FeCrAlY mesh with dimensions of  $27 \times 27$  mm was used as a substrate for wash-coating the catalyst. A fresh FeCrAlY mesh was heat-treated at  $900^\circ C$  for 2 h in air. The treated mesh was coated with a Zr solution followed by heat treatment at  $700^\circ C$  in air for 2 h. The Pt catalyst was coated on the Zr-coated FeCrAlY mesh and calcined at  $300^\circ C$  for 2 h. As shown in Fig. 1, the prepared FeCrAlY mesh was rolled carefully and installed at the combustion outlet conduit.

### 2.2. Design of microchannel heat exchanger

Plate-type heat-exchangers were used to recover the heat of the combustion and reformed gases. Furthermore, the recovered heat was used to preheat the reactant gases, e.g., air and methane, and to vapourize the liquid water. The microchannel heat-exchanger for preheating air consists of a cover plate, a base plate and five sets (10 plates) microchannel sheets. The microchannel heat-exchanger for preheating methane and vapourizing water consists of a cover plate, a base plate and 25 sets (50 plates) microchannel sheets. A stainless-steel plate was used to fabricate the microchannel sheets, as well as the cover

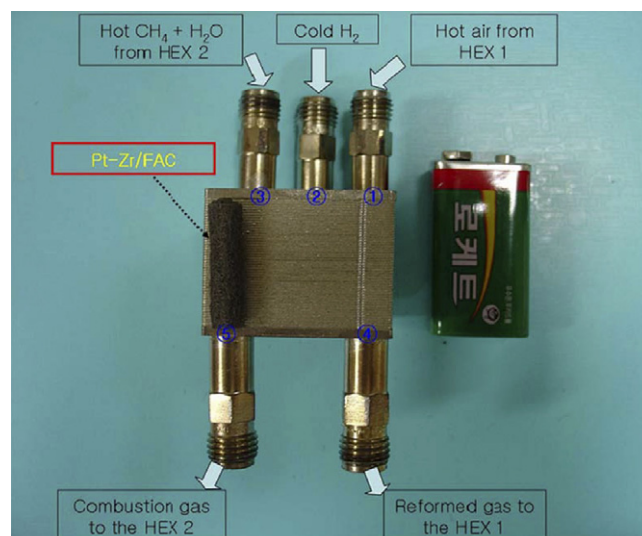


Fig. 1. Igniter (Pt–Zr/FAC) equipped with a microchannel reactor for rapid start-up. Numbers indicate points at which temperature is measured.

and the base plates. Microchannels were patterned on metal plates using a wet chemical-etching method. Each microchannel sheet had two conduits and two flow-distribution chambers to provide uniform gas distribution. Each sheet with 34 channels had the following flow path dimensions:  $300 \mu m$  in diameter,  $30 \mu m$  in depth, and 20 mm in length. Two types of sheet, which were a mirror image of each other, were stacked alternately and bonded by a brazing method. The two types of sheet are shown in Fig. 2. The dimensions of heat-exchanger 1 and heat-exchanger 2, excluding the fittings, were approximately  $40 \times 40 \times 7$  mm and  $40 \times 40 \times 27$  mm, respectively. The assembled units of the microchannel heat-exchanger 1 and heat-exchanger 2 are shown in Fig. 3.

### 2.3. Hydrogen catalytic combustion and methane steam reforming

The microchannel reactor used in this study was the same as that reported elsewhere [10]. A stoichiometric mixture of hydro-

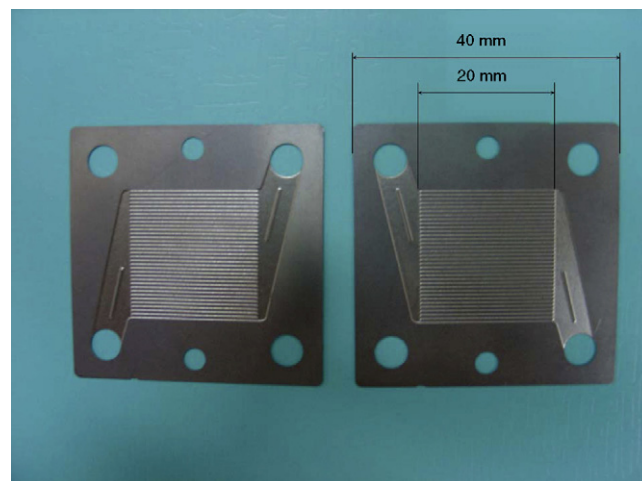


Fig. 2. Two types of microchannel sheets used in heat-exchanger. Each sheet is a mirror image of the other.

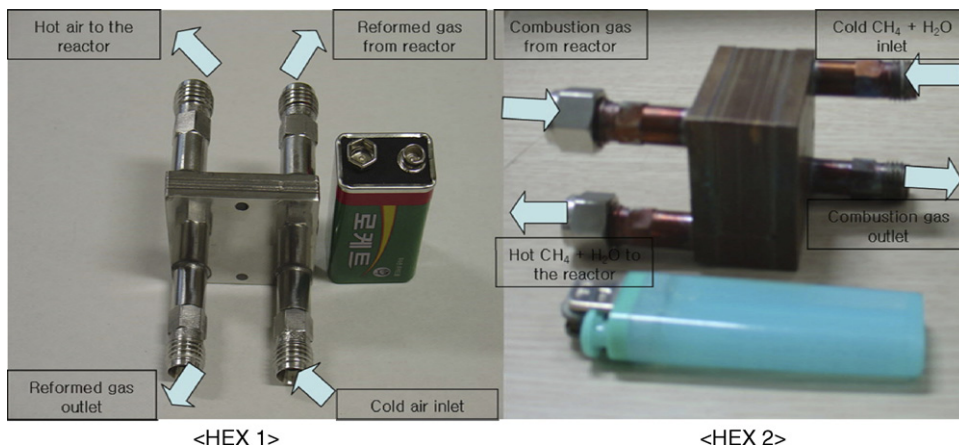


Fig. 3. Assembled unit of microchannel heat-exchanger 1 (for preheating air) and heat-exchanger 2 (for preheating methane and vapourizing water).

gen and air were introduced for combustion. Hydrogen was introduced into the newly designed conduit, as explained earlier [10]. Air was pre-heated in the microchannel heat-exchanger 1. Methane and liquid water were supplied into the microchannel heat-exchanger 2 for methane steam reforming. The temperature was controlled by regulating the flow rate of the hydrogen and air mixture. Methane steam reforming tests were carried out at a steam-to-carbon ratio of 3.0. A detail schematic diagram of the experimental set-up is reported elsewhere [10]. The gas was supplied by a mass-flow controller (MFC, Brooks 5850 series) and liquid water was supplied by a micro liquid pump (NS, MINICHEMI PUMP,  $1\text{--}1000\ \mu\text{l min}^{-1}$ ). The water was introduced at a heat-exchanger 2 temperature of  $120\ ^\circ\text{C}$ . The liquid components were separated by a cold trap in the produced stream. The flow rate of the reformed gas was measured using a soap bubble flow meter. The reactants and products gases were analyzed with a gas chromatograph (Agilent 6890N) that was equipped with HP-MOLSIV, HAYESEP D columns and thermal conductivity detectors (TCD). The temperature was monitored using a data-acquisition/switch unit (Agilent 34790A) that was equipped with K type thermocouple placed into every conduit in the reactor. The position at which the temperature was measured are shown in Fig. 1. The microchannel fuel processor with the heat-exchangers was insulated with ceramic wool before conducting tests.

### 3. Results and discussion

#### 3.1. Fast start-up of microchannel fuel processor

Hydrogen combustion takes place over a platinum catalyst, even at room temperature [23,25]. Although the hydrogen and oxygen reaction is very fast and there is a broad explosion limit for hydrogen (4–94% in  $\text{O}_2$  on a volume percent basis), the problems associated with this explosive reaction can be solved by using a microchannel reactor. The MCR can suppress propagation of flames because the dimensions of the microchannels ( $500 \times 250\ \mu\text{m}$ ) are smaller than the quenching distance for  $\text{H}_2/\text{O}_2$  mixtures, which is approximately  $1000\ \mu\text{m}$  [10,23,26]. A high catalyst load is need for the dynamic process [23], but is difficult to place a high catalyst load on microchannel sheets

made from metals. The FeCrAlY mesh is a good solution to this problem. A high catalyst load can be deposited on the mesh on account of its very high surface-to-volume ratio. Furthermore, the mesh has similar thermal conductivity to that of the microchannel plate and there by allows rapid transfer of heat.

A coating of the Pt–Zr, to serve as a combustion catalyst, was applied to the FeCrAlY mesh. The prepared FeCrAlY mesh was rolled carefully so it could be installed into the one of the conduits of microchannel reactor as an igniter for hydrogen combustion. Hydrogen is extremely light compared with air and flows/diffuses upward across the catalyst body [22]. The rolled Pt–Zr/FeCrAlY mesh was installed into the combustion outlet side of the microchannel reactor. The mesh induced ignition at the end of combustion section and allowed movement of the hot spot to the microchannel of the combustion section. A thermocouple was placed immediately below the rolled Pt–Zr/FeCrAlY mesh and its tip touched the Pt–Zr/FeCrAlY mesh. The hydrogen flow rate was varied from  $0.022$  to  $0.054\ \text{mol min}^{-1}$ . A mass flow controller was used to introduce a stoichiometric volume of air. Nitrogen ( $4.9 \times 10^{-3}\ \text{mol min}^{-1}$ ) and water ( $1.5 \times 10^{-2}\ \text{mol min}^{-1}$ ) were introduced into the reforming section.

As shown in Fig. 4, the rate of temperature increase in the microchannel reactor is very fast and the maximum temperature increases with increasing hydrogen flow rate. In all cases, the microchannel reactor heats up to the working temperature within a minute. After the temperature reaches the maximum point, it decreases because the hydrogen diffuses upwards across the rolled Pt–Zr/FeCrAlY mesh body. After a few minutes, the temperature increases slowly and reached the first maximum point. This microchannel reactor can be heated up within a minute by introducing the Pt–Zr/FeCrAlY mesh as an igniter for hydrogen combustion. It is anticipated that this type of reactor can be applied to a dynamic process such a portable fuel processor and/or liquid, e.g., methanol, vapourizer.

#### 3.2. Effect of heat-exchanger on reactor capacity and energy efficiency

It is well known that the major gas products of methane steam reforming are hydrogen and carbon monoxide, reaction

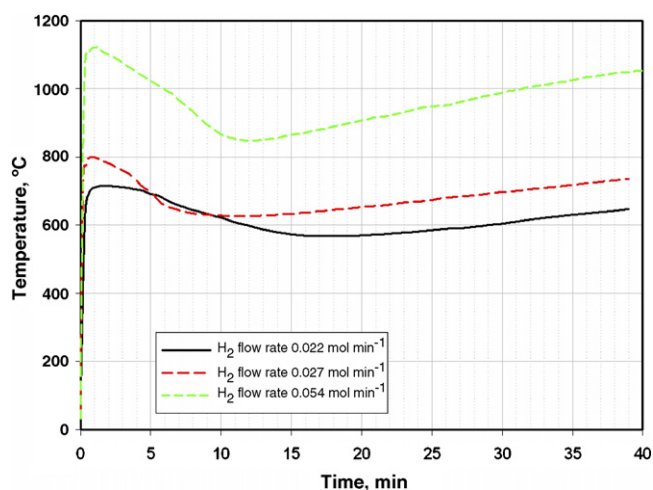
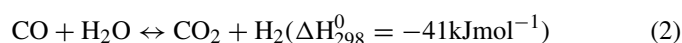
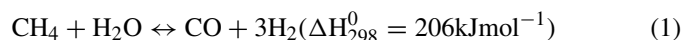


Fig. 4. Temperature profiles in combustion outlet conduit. The thermocouple is placed immediately below the Pt–Zr coated FAC roll (point 5).

(1). A small concentration of carbon dioxide is produced via the water–gas shift (WGS) reaction (2):



Reactions (1) and (2) can be summarized as follows (3):



A high concentration of hydrogen and a low concentration of carbon monoxide are desirable for PEMFC applications. In order to improve the hydrogen and carbon dioxide selectivity, it is beneficial to increase the steam-to-carbon ratio (S:C ratio). An increase in the S:C ratio means that a higher heat flux is required to evaporate the additional water in the feed stream. For this reason, there is a need for a compromise between selectivity and system efficiency. In addition, a molar steam-to-carbon ratio of 3.0 must be maintained in order to inhibit carbon precipitation.

The composition of product gas at different reforming temperatures is given in Fig. 5. Methane was introduced at a rate of  $5 \times 10^{-3} \text{ mol min}^{-1}$  with a S:C ratio of 3.0. The MCR temper-

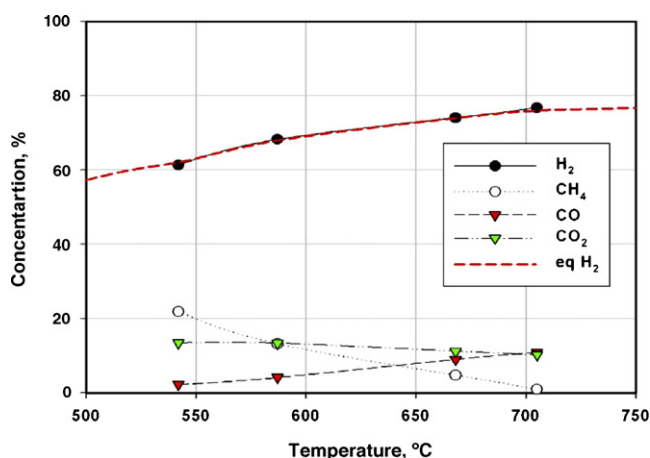


Fig. 5. Effect of reformer outlet temperature on composition of dry reformate.  $\text{CH}_4$  feed flow rate =  $5.0 \times 10^{-3} \text{ mol min}^{-1}$ , steam-to-carbon ratio = 3.0.

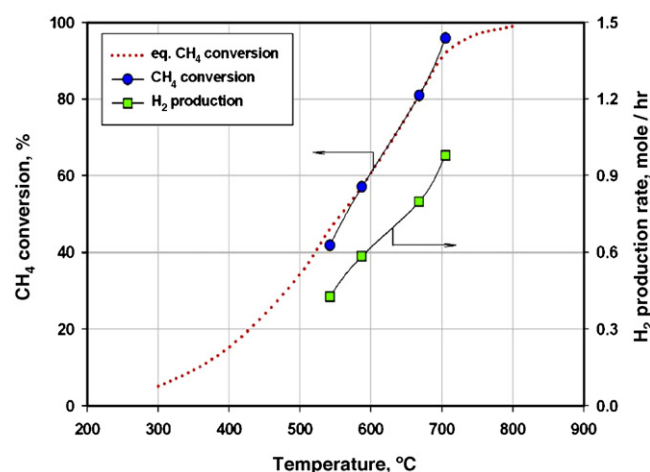


Fig. 6.  $\text{CH}_4$  conversion and  $\text{H}_2$  production rate according to reformer outlet temperature.  $\text{CH}_4$  feed flow rate =  $5.0 \times 10^{-3} \text{ mol min}^{-1}$ , steam-to-carbon ratio = 3.0.

ature controlled by varying the hydrogen/air flow rate. As the reformer outlet temperature is increased from 542 to 705 °C, the concentration of  $\text{H}_2$  increases from 61 to 77 volumetric %, as shown in Fig. 5, and is similar to the equilibrium value. This indicates that the MCR has excellent heat and mass-transfer characteristics. The concentration of CO also increases with temperature. Since this concentration should be less than 20 ppm for application in fuel cells, additional CO clean-up processes such as the WGS reaction, partial oxidation and/or methanation are required to reduce the CO concentration, to an acceptable level.

The  $\text{CH}_4$  conversion and  $\text{H}_2$  production rate for a constant rate of feed demonstrate the performance of the fuel processor. The rates of  $\text{CH}_4$  conversion and  $\text{H}_2$  production according to the reformer outlet temperature are presented in Fig. 6. Both these rates increase with increasing reformer outlet temperature. At 705 °C, the rates of  $\text{CH}_4$  conversion and  $\text{H}_2$  production are 96% and  $9.8 \times 10^{-1} \text{ mol h}^{-1}$ , respectively. Furthermore, the rate of  $\text{CH}_4$  conversion is very similar to the equilibrium value. These findings show that the reformer with microchannels sustains very fast molecular diffusion. The electrical power for a typical fuel cell can be obtained with 60% efficiency and 80% utilization of  $\text{H}_2$ . According to this assumption, the anticipated power outlet of the MCR reformer is about 31 W as fuel cell power.

The  $\text{CH}_4$  conversion and  $\text{H}_2$  production rates together with the temperature profile for reforming are shown in Fig. 7 as a function of the feed flow-rate; the test conditions for each case are given in Table 1. The data show that hydrogen production

Table 1  
Conditions of combustion and methane steam reforming

| Case | Combustion section                     |   | Reforming section                                |  |
|------|--|---|--|--|
|      | Air ( $10^{-2} \text{ mol min}^{-1}$ ) | $\text{H}_2$ ( $10^{-2} \text{ mol min}^{-1}$ ) | $\text{CH}_4$ ( $10^{-2} \text{ mol min}^{-1}$ ) | Steam ( $10^{-2} \text{ mol min}^{-1}$ ) |
| 1    | 9.38                                   | 3.75  | 0.25   | 0.75                                     |
| 2    | 12.0                                   | 4.80  | 0.50   | 1.55                                     |
| 3    | 15.5                                   | 6.20  | 1.00   | 3.00                                     |
| 4    | 19.3                                   | 7.65  | 1.70   | 5.10                                     |

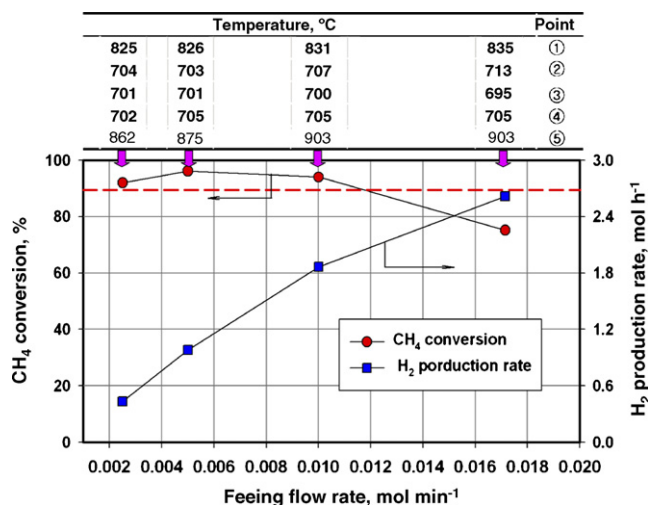


Fig. 7. CH<sub>4</sub> conversion and H<sub>2</sub> production rate, and temperature profile for reforming as function of feed flow-rate. Steam-to-carbon ratio=3.0. Dashed line is equilibrium methane conversion rate at 700 °C.

increases with increasing methane-feeding rate. Furthermore, with the heat-exchanger, the reforming capacity of the reactor is enhanced by about 3.4 times compared with that reported in a previous study [10]. On the other hand, the temperature gradient between the combustion and reforming sections ranges from 160 to 200 °C. As shown in the Table given in Fig. 7, the temperature gradient increases with the extent of the more methane steam reforming reaction. This is because methane steam reforming is a highly endothermic reaction. The energy balance and reactor performance is shown in Table 2. It can be seen that the energy efficiency increases with increasing methane feed rate. Furthermore, the energy efficiency is enhanced by a factor of 1.8 with the heat-exchanger, as compared with the previous study [10].

On other hand, the amount of hydrogen consumed is 1.7 times higher than that produced by the methane steam reforming due to the low thermal content of hydrogen. Hence, it is necessary to conduct further experiments with a mixture of methane and hydrogen as a fuel for catalytic combustion.

### 3.3. New design concept of heat-exchanger integrated micro fuel processor and fuel cell system

A new device with longer channels and a reduced plate width was designed by applying the results obtained from heat-exchangers with the integrated microchannel fuel processor. The design of this new device is presented in Fig. 8. A heat-exchanger is placed at the top and the bottom of the microchannel reformer. Furthermore, in order to increase the surface area for a high catalyst loading, one of the plates between the reforming and combustion sections has three-dimensional channels, i.e., mesh type. In this design, plates with three-dimensional channels can be placed in the combustion section to increase the surface area for a high catalyst loading. However, the quenching distance of hydrogen combustion needs to be considered when installing a three-dimensional channel plate in the combustion section. Furthermore, the channel length of the plate has to be increased and the width of the plate has to be reduced in order to improve the heat-exchanger efficiency. Delsman et al. [18] reported that a micro device with longer channels and a narrow width could improve the heat-exchanger efficiency with a lower number of plates. Numerical modelling and experiments can be used to determine the number of plates in each section.

A prospective new design of fuel-cell system is shown in Fig. 9. The excess hydrogen generated from hydrocarbon reforming is stored in a tank and used as a start-up fuel for fuel processor. After start-up, fuel can be changed from hydrogen to

Table 2  
Energy balance and performance of developed fuel processor

| Case | Reaction                    | Flow rate (10 <sup>-2</sup> mol min <sup>-1</sup> ) | Conversion (%) | Portion (%) | Total $\Delta H_{298}^0$ (kJ h <sup>-1</sup> ) |
|------|-----------------------------|---|----------------|-------------|--|
| 1    | H <sub>2</sub> combustion   | 3.75  | 100            | 100         | -545   |
|      | 1                           | 0.25  | 91             | 65          | 18   |
|      | 3                           | 0.25  |                | 35          | 8  |
|      | H <sub>2</sub> regeneration | 0.7   |                |             | 104  |
|      | Efficiency                  |   |                | 23.9%       |  |
| 2    | H <sub>2</sub> combustion   | 4.80  | 100            | 100         | -697   |
|      | 1                           | 0.5   |                | 52          | 31   |
|      | 3                           | 0.5   | 96             | 48          | 23   |
|      | H <sub>2</sub> regeneration | 1.7   |                |             | 237  |
|      | Efficiency                  |   |                | 41.7%       |  |
| 3    | H <sub>2</sub> combustion   | 6.20  | 100            | 100         | -900   |
|      | 1                           | 1.0   |                | 55          | 64   |
|      | 3                           | 1.0   | 94             | 45          | 42   |
|      | H <sub>2</sub> regeneration | 3.1   |                |             | 453  |
|      | Efficiency                  |   |                | 62.0%       |  |
| 4    | H <sub>2</sub> combustion   | 7.65  | 100            | 100         | -1100  |
|      | 1                           | 1.7   |                | 48          | 73   |
|      | 3                           | 1.7   | 73             | 52          | 64   |
|      | H <sub>2</sub> regeneration | 4.4   |                |             | 634  |
|      | Efficiency                  |   |                | 69.4%       |  |

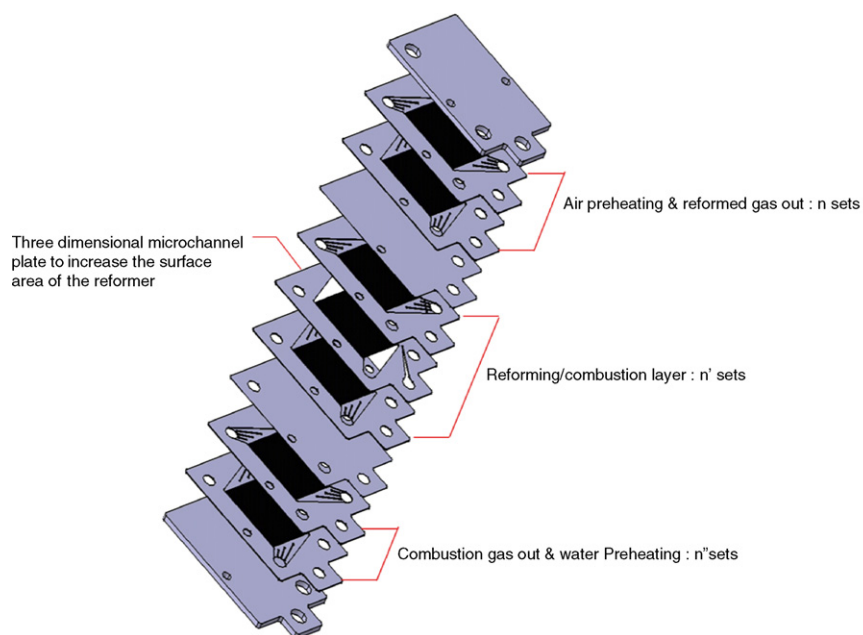


Fig. 8. Schematic drawing of heat-exchanger integrated fuel processor. Three dimensional microchannel plates are installed between combustion plate and reforming plate to increase surface area of reforming plate.

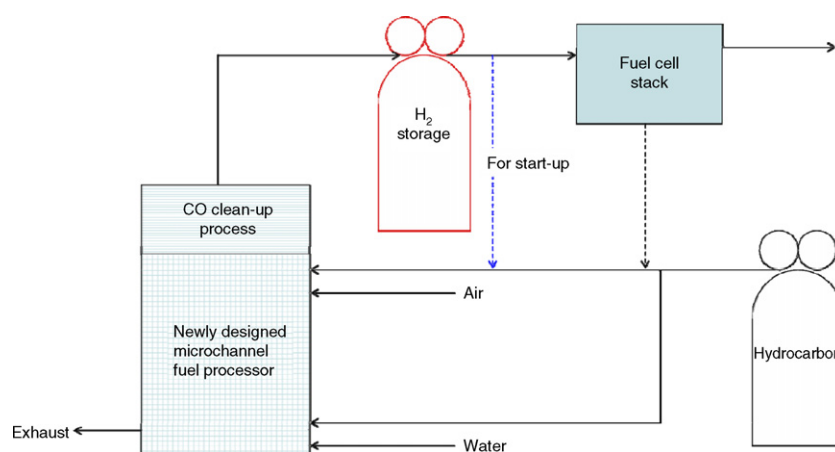


Fig. 9. Schematic drawing of newly designed system for steam reforming. A hydrogen storage tank is installed between the CO clean-up process and the fuel cell stack for start-up fuel.

methane, other hydrocarbon material, or a mixture of hydrogen and hydrocarbon. This fuel-cell system concept can allow further advances in the development of a simple system to remove the need for an electro device to start-up the fuel processor.

#### 4. Conclusions

This study examines hydrogen combustion and methane steam reforming in a plate-type heat-exchanger contained in an integrated microchannel fuel processor. The introduction of Pt–Zr/FaCrAlY mesh as an igniter of hydrogen combustion allows this microchannel reactor to be operational within a minute. This type of reactor can be applied to a dynamic process such as a portable fuel processor and/or liquid, e.g., methanol, vapourizer.

By introducing plate-type heat-exchangers, the reactor capacity of the methane steam reforming and the energy efficiency can be enhanced by factors of about 3.4 and 1.8, respectively. Energy balance analysis shows, however that the amount of hydrogen consumed is 1.7 times higher than that produced by methane steam reforming because of the low thermal content of hydrogen. Therefore, further experiments are required with a mixture of methane and hydrogen as a fuel for catalytic combustion.

Using this type of reactor concept, a new microchannel device and fuel-cell system can be designed, in which a plate-type heat-exchanger is integrated into a single device. In addition, a new three-dimensional microchannel plate can be installed in the reforming and/or combustion section to increase the surface-to-volume ratio. This concept can allow further advances in the development of compact and dynamic fuel processors. In the

new fuel-cell system, hydrogen is stored in a tank to provide the start-up fuel. This fuel-cell system offers further advances in the development of a simple system without an electro device to start-up the fuel processor.

### Acknowledgements

The research was sponsored by the Center for Environmentally Friendly Vehicle (CEFV) as an Eco-STAR Project, in the Korean Government's R&D Program on environmental technology development.

### References

- [1] G. Kolb, V. Hessel, *Chem. Eng. J.* 98 (2004) 1–38.
- [2] G. Vesper, *Chem. Eng. Sci.* 56 (2001) 1265–1273.
- [3] Y. Chin, J. Hu, C. Cao, Y. Gao, Y. Wang, *Catal. Today* 110 (2005) 47–52.
- [4] S.-H. Lee, K. Miyazawa, R. Maeda, *Carbon* 43 (2005) 855–894.
- [5] J. Wagner, T. Kirner, G. Mayer, J. Albert, J.M. Kohler, *Chem. Eng. J.* 101 (2004) 251–260.
- [6] M. Saito, L.-J. Yin, I. Kobayachi, M. Nakajima, *Food Hydrocolloids* 19 (2005) 745–751.
- [7] S. Sugiura, M. Nakajima, J. Tong, H. Nabetani, M. Seki, *J. Colloid Interface Sci.* 227 (2000) 95–103.
- [8] Z. Chen, A. Chauhan, *J. Colloid Interface Sci.* 285 (2005) 834–844.
- [9] M.J. Mahoney, R.R. Chen, J. Tan, W.M. Saltzman, *Biomaterials* 26 (2005) 771–778.
- [10] S.-K. Ryi, J.-S. Park, S.-H. Choi, S.-H. Cho, S.-H. Kim, *Chem. Eng. J.* 113 (2005) 47–53.
- [11] A.S. Patil, T.G. Dubois, N. Sifer, E. Bostic, K. Gardner, M. Quah, C. Bolton, *J. Power Sources* 136 (2004) 220–225.
- [12] A.Y. Tonkovich, S. Perry, Y. Wang, D. Qiu, T. Laplant, W.A. Rogers, *Chem. Eng. Sci.* 59 (2004) 4819–4824.
- [13] Y. Men, H. Gnaser, R. Zapf, V. Hessel, C. Ziegler, G. Kolb, *Appl. Catal. A: Gen.* 277 (2004) 83–90.
- [14] I. Aartun, B. Silberova, H. Venvik, P. Pfeifer, O. Gorke, K. Shubert, A. Holman, *Catal. Today* 105 (2005) 469–478.
- [15] I. Aartun, T. Gjervan, H. Venvik, O. Gorke, P. Pfeifer, M. Fathi, A. Holmen, K. Schubert, *Chem. Eng. J.* 101 (2004) 93–99.
- [16] O. Goerke, P. Pfeifer, K. Schubert, *Appl. Catal.* 263 (2004) 11–18.
- [17] A.Y. Tonkovich, J.L. Zilka, M.J. LaMont, Y. Wang, R.S. Weneng, *Chem. Eng. Sci.* 54 (1999) 2947–2951.
- [18] E.R. Delsman, M.H.J.M. De Croon, A. Pierik, G.J. Kramer, P.D. Cobden, Ch. Hofmann, V. Cominos, J.C. Schouten, *Chem. Eng. Sci.* 59 (2004) 4795–4802.
- [19] E.R. Delsman, M.H.J.M. De Croon, G.J. Kramer, P.D. Cobden, Ch. Hofmann, V. Cominos, J.C. Schouten, *Chem. Eng. J.* 101 (2004) 123–131.
- [20] G. Chen, Q. Yuan, H. Li, S. Li, *Chem. Eng. J.* 101 (2004) 101–106.
- [21] D.R. Palo, J.D. Holladay, R.T. Rozmiarek, C.E. Guzman-Leong, Y. Wang, J. Hu, Y.-H. Chin, R.A. Dagle, E.G. Baker, *J. Power Sources* 108 (2002) 28–34.
- [22] M. Haruta, H. Sano, *Int. J. Hydrogen Energy* 7 (1982) 737–740.
- [23] M.T. Janicke, H. Kestenbaum, U. Hagendorf, F. Schuth, M. Fichtner, K. Schubert, *J. Catal.* 191 (2000) 282–293.
- [24] V. Yakhnin, M. Menzinger, *Chem. Eng. Sci.* 57 (2002) 4559–4567.
- [25] M. Haruta, H. Sano, *Int. J. Hydrogen Energy* 6 (1981) 601–608.
- [26] B. Lweis, G. von Elbe, *Combustion and Flames and Explosions of Gases*, Academic Press, New York, USA, 1987.